

# Advanced Nonlinear SCMA Codebook Design Based on Lattice Constellation

Qu Luo, *Member, IEEE*, Jing Zhu, *Member, IEEE*, Gaojie Chen, *Senior Member, IEEE*, Pei Xiao, *Senior Member, IEEE*, Rahim Tafazolli, and Fan Wang.

**Abstract**—The design of efficient sparse codebooks in sparse code multiple access (SCMA) system have attracted tremendous research attention in the past few years. This paper proposes a novel nonlinear SCMA (NL-SCMA) that can subsume the conventional SCMA system which is referred to as linear SCMA, as special cases for downlink channels. This innovative approach allows a direct mapping of users' messages to a superimposed codeword for transmission, eliminating the need of a codebook for each user. This mapping is referred to as nonlinear mapping (codebook) in this paper. Hence, the primary objective is to design the nonlinear mapping, rather than the linear codebook for each user. We leverage the Lattice constellation to design the superimposed constellation due to its advantages such as the minimum Euclidean distance (MED), constellation volume, design flexibility and shape gain. Then, by analyzing the error patterns of the Lattice-designed superimposed codewords with the aid of the pair-wise error probability, it is found that the MED of the proposed nonlinear codebook is lower bounded by the “single error pattern”. To this end, an error pattern-inspired codebook design is proposed, which can achieve large MEDs of the nonlinear codebooks. Numerical results show that the proposed codebooks can achieve lower error rate performance over both Gaussian and Rayleigh fading channels than the-state-of-the-art linear codebooks.

**Index Terms**—Sparse code multiple access (SCMA), nonlinear SCMA (NL-SCMA), codebook design, Lattice constellation.

## I. INTRODUCTION

THE ever-increasing demand for higher data rates, improved spectral efficiency, and massive connectivity has driven the rapid evolution of wireless communication systems [1]. To meet these requirements, non-orthogonal multiple access (NOMA) technique has been envisioned as a promising technique for future wireless communication networks [1], [2]. Distinguished from conventional orthogonal multiple access (OMA) technologies such as time division multiple access and orthogonal frequency division multiple access, NOMA enables the transmission of multiple users over the same time-frequency resources [2]. Until now, many NOMA schemes have been proposed, including power-domain NOMA (PD-NOMA) [3], multiuser shared access (MUSA) [4], pattern division multiple access (PDMA) [5], interleave-grid multiple access (IGMA) [6] and code-domain NOMA (CD-NOMA)

[7]. In particular, sparse code multiple access (SCMA) is a representative CD-NOMA scheme, which carries out multiplexing by employing carefully designed codebooks/sequence [8]. In SCMA, each user is assigned an unique codebook, and the incoming message bits from the user are directly mapped to a multi-dimensional codeword, which is intentionally sparse so as to reduce the decoding complexity by employing the message passing algorithm (MPA) [9]–[12]. The multi-dimensional codeword also provides a constellation shape gain and consequently leads to better spectral efficiency when compared to other CD-NOMA schemes such as low density spreading code division multiple access (LDS-CDMA) and low density signature-orthogonal frequency division multiplexing (LDS-OFDM) [13].

### A. Related works

A fundamental research problem in SCMA is how to design efficient sparse codebook for low error rate transmission and by now, the SCMA codebook design has acquired the status of an open problem [2], [14]–[23]. Current codebook design approaches typically follow a top-down methodology by first constructing a mother constellation (MC), upon which certain user-specific operators, such as phase rotation and permutation, are applied to the MC to obtain codebooks for multiple users [2], [15]–[21]. The design key performance indicators (KPIs) for the MC and user-specific operators are generally the the minimum product distance (MPD) and the the minimum Euclidean distance (MED) of the MC, and the MED of the superimposed constellation [2]. In general, a large MED leads to reliable detection in the Gaussian channel, whereas a large MPD is preferred for robust transmissions in the Rayleigh fading channels.

Following the top-down idea, the pulse amplitude modulation (PAM) constellation and golden angle modulation constellation (GAM) were considered as the MC in [15] and [17], respectively, where the MED of the MC is considered as the KPI in downlink SCMA systems. The 4-PAM constellation was also adopted in [18], [19] for large capacity, energy efficiency and mutual information gain. It is noted that the same 4-order PAM constellation was employed as the basic constellation in [18], [19], thus their resultant codebooks exhibit certain similarity. In [22], power-imbalanced codebooks were proposed by maximizing the MED of the superimposed constellation while maintaining the MPD of the MC larger than a threshold. In [24], the authors considered Star-QAM as the MC for enlarged MED of the superimposed

This work was supported by the U.K. Engineering and Physical Sciences Research Council under Grant EP/P03456X/1 and EP/X013162/1. (Corresponding author: Qu Luo)

Q. Luo, J. Zhu, G. Chen and P. Xiao are with 5G and 6G Innovation centre, Institute for Communication Systems (ICS) of University of Surrey, Guildford, GU2 7XH, U.K. (e-mail: {q.u.luo, j.zhu, gaojie.chen, p.xiao, r.tafazolli}@surrey.ac.uk). Fan Wang was with Huawei Technologies Company Ltd. (email: fan.wang@huawei.com)

codewords in downlink SCMA systems. In [16], near-optimal codebooks for different channel conditions were investigated by choosing suitable MCs with large MPD or MED. More recently, a comprehensive approach to achieve near-optimal SCMA codebooks designs for 150% and 200% overloading factors under various channel environments was studied in [20].

There are yet other works combining constellation to design SCMA codebooks. The author in [21] proposed an uniquely decomposable constellation group with amplitude and phase-shift keying modulation. In addition, a joint design of codebook and peak-to-average power ratio (PAPR) reduction based on the partial transmit sequence technique was proposed in [25]. Different from the above works, which mainly design the codebooks over Gaussian or Rayleigh fading channels, the recent work in [2] studied the codebook design in Ricain fading channels, where a novel class of low-projection SCMA codebooks for ultra-low decoding complexity was developed. As revealed by many SCMA works [2], [14], [16], [18]–[21], [26], the distance properties of the superimposed constellation, such as the MED of the superimposed constellation, the MED at each resource node, the volume of the constellation at each subcarrier, the PAPR of the superimposed constellation, play an essential role in improving the performance of SCMA systems.

### B. Motivation and Contribution

One fundamental characteristic of the above SCMA codebook design is the utilization of an MC to generate the multi-dimensional codebook based on the top-down principle. Thus, the performance of the codebook relies heavily on the selection of an MC and the user-specific constellation operators [2], [14], [16], [18]–[21], [26]. Numerous studies on SCMA have highlighted the crucial role of the the superimposed constellation, such as the MED [14], [16], [18], [20], [21], the MED at each subcarrier [16], [20], the volume of the constellation at each subcarrier [18], [26]. However, designing a codebook that simultaneous achieves these objectives poses a considerable challenge to the existing design schemes. An alternative and more ambitious approach is to directly design the superimposed constellation with desirable characteristics instead of following a top-down based principle. This is reasonable as the user bit message can be uniquely determined by the superimposed constellation as long as the superimposed constellation is well designed [2].

In this paper, a novel nonlinear SCMA (NL-SCMA) is proposed, where the input message of SCMA users are directly mapped to the superimposed codeword according to a specific nonlinear mapping rule. The mapping process is referred to as nonlinear codebook (NLCB) in this paper, whereas the conventional SCMA codebook is thus called linear codebook (LCB). Motivated by the superiority of the Lattice constellation, such as the large shape gain, large MED, good design flexibility and superior performance [27], we employ the Lattice constellation to design the superimposed constellation. As such, the resultant superimposed constellation can also enjoy these benefits [27]. The main contributions of this work can be summarized as follows:

- We propose a NL-SCMA system that directly maps the input message of SCMA users to the superimposed codeword. The proposed NL-SCMA can serve as a general framework and subsumes the existing linear SCMA systems as special cases.
- A constellation partition scheme is proposed to design the superimposed constellation at each subcarrier based on the Lattice constellation, where the partitioned constellation is called Lattice code.
- We propose an error-pattern inspired method to design the nonlinear mapping between the input message and the multi-dimensional superimposed codeword by exploiting the unique characteristic of the pair-wise error probability (PEP) of the proposed NL-SCMA. Hence, the proposed scheme is referred to as error-pattern inspired NLCB design.
- We conduct extensive numerical experiments to show the superiority of the proposed linear and NL-SCMA codebooks. Numerical results indicate that the proposed codebooks can simultaneous achieve lower error rate performance in uncoded and coded systems and large MED than the-state-of-the-art codebooks.

### C. Organization

The remainder of this paper are outlined as follows. Section II introduces the system model of linear SCMA and the proposed NL-SCMA systems. The SCMA codebook design KPIs are illustrated in Section III, followed by the brief introduction of existing linear SCMA designs. In Section IV, the detailed design of the NL-SCMA and LCBs are discussed. Section V is the numerical results, followed by the conclusions in Section VI

### D. Notation

$\mathbb{C}^{k \times n}$  and  $\mathbb{B}^{k \times n}$  denote the  $(k \times n)$ -dimensional complex and binary matrix spaces, respectively.  $\mathbf{I}_n$  denotes an  $n \times n$ -dimensional identity matrix.  $\text{diag}(\mathbf{x})$  gives a diagonal matrix with the diagonal vector of  $\mathbf{x}$ .  $(\cdot)^T$ ,  $(\cdot)^\dagger$  and  $(\cdot)^H$  denote the transpose, the conjugate and the Hermitian transpose operation, respectively.  $\|\mathbf{x}\|_2$  and  $|x|$  return the Euclidean norm of vector  $\mathbf{x}$  and the absolute value of  $x$ , respectively.  $\mathcal{CN}(0, 1)$  denotes the complex distribution with zero mean and unit variance.

## II. SYSTEM MODEL

### A. SCMA Communication Model

We consider a downlink SCMA system, where  $J$  users (UEs) communicate over  $K$  orthogonal subcarriers. The overloading factor defined as  $J/K$  is larger than one. In SCMA, each user is assigned with an unique codebook, denoted by  $\mathcal{X}_j = \{\mathbf{x}_{j,1}, \mathbf{x}_{j,2}, \dots, \mathbf{x}_{j,M}\} \in \mathbb{C}^{K \times M}$ ,  $j \in \{1, 2, \dots, J\}$ , where  $M$  is the codebook size and  $\mathbf{x}_{j,m}$  is the  $m$ th codeword with a dimension of  $K$ . During transmissions, each user maps  $\log_2(M)$  binary bits to a length- $K$  codeword  $\mathbf{x}_j$  drawn from the  $\mathcal{X}_j$ . The mapping process can be expressed as [28]

$$f_j : \mathbb{B}^{\log_2 M \times 1} \rightarrow \mathcal{X}_j \in \mathbb{C}^{K \times M}, \text{ i.e., } \mathbf{x}_j = f_j(\mathbf{b}_j), \quad (1)$$

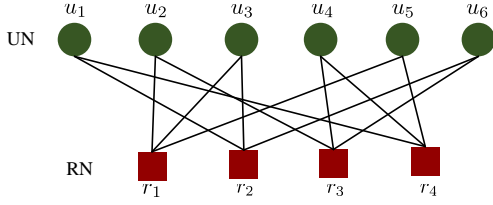


Fig. 1: Factor graph representation of a SCMA system.

where  $\mathbf{b}_j = [b_{j,1}, b_{j,2}, \dots, b_{j, \log_2 M}]^T \in \mathbb{B}^{\log_2 M \times 1}$  represents the binary message input for the  $j$ th user. The  $K$ -dimensional complex codewords in the SCMA codebook are sparse vectors with  $N$  non-zero elements and  $N < K$ . The factor graph can be used to represent the connections between user nodes (UNs) and resource nodes (RNs) in SCMA. The sparse structure of the  $J$  SCMA codebooks can also be represented by the indicator matrix  $\mathbf{F}_{K \times J} \in \mathbb{B}^{K \times J}$ . An element of  $\mathbf{F}$  is defined as  $f_{k,j}$  which takes the value of 1 if and only if UN  $u_j$  is connected to RN  $r_k$  and 0 otherwise. In this paper, the following indicator matrix with  $J = 6$ ,  $K = 4$  and  $N = 2$  is considered [28]:

$$\mathbf{F}_{4 \times 6} = \begin{bmatrix} 0 & 1 & 1 & 0 & 1 & 0 \\ 1 & 0 & 1 & 0 & 0 & 1 \\ 0 & 1 & 0 & 1 & 0 & 1 \\ 1 & 0 & 0 & 1 & 1 & 0 \end{bmatrix}, \quad (2)$$

where the factor graph representation is shown in Fig. 1.

Let  $\mathbf{c}_j$  be a length- $N$  vector drawn from  $\mathcal{C}_j \subset \mathbb{C}^{N \times 1}$ , where  $\mathcal{C}_j$  is obtained by removing all the zero elements in  $\mathcal{X}_j$ . We further define the mapping from  $\mathbb{B}^{\log_2 M \times 1}$  to  $\mathcal{C}_j$  as [17]

$$q_j : \mathbb{B}^{\log_2 M \times 1} \mapsto \mathcal{C}_j, \quad \text{i.e., } \mathbf{c}_j = q_j(\mathbf{b}_j). \quad (3)$$

Thus, the corresponding SCMA mapping  $v_j$  can be expressed as

$$v_j : \mathbf{V}_j q_j \mapsto \mathcal{X}_j, \quad \text{i.e., } \mathbf{x}_j = \mathbf{V}_j q_j(\mathbf{b}_j), \quad (4)$$

where  $\mathbf{V}_j \in \mathbb{B}^{K \times N}$  is a mapping matrix that maps the  $N$ -dimensional vector to a  $K$ -dimensional sparse SCMA codeword. Based on the factor graph,  $\mathbf{V}_j$  can be constructed according to the position of the '0' elements of  $\mathbf{f}_j$  by inserting all-zero row vectors into the identity matrix  $\mathbf{I}_N$ .

For example, we have  $\mathbf{V}_1 = \begin{bmatrix} 0 & 1 & 0 & 0 \\ 0 & 0 & 0 & 1 \end{bmatrix}^T$  and  $\mathbf{V}_2 = \begin{bmatrix} 1 & 0 & 0 & 0 \\ 0 & 0 & 1 & 0 \end{bmatrix}^T$ , and  $\mathbf{V}_j, j = 3, 4, 5$  and 6 can be generated in a similar way.

For a downlink SCMA system, the transmitted codeword of each user is first superimposed at the base station, leading to a superimposed codeword, denoted by  $\mathbf{w} = [w_1, w_2, \dots, w_K]^T \in \mathbb{C}^{K \times 1}$ . Namely, we have [17]

$$\mathbf{w} = \sum_{j=1}^J \mathbf{x}_j. \quad (5)$$

### B. The Proposed NL-SCMA

In existing SCMA systems, the transmitted vector  $\mathbf{w}$  is obtained by combining the codewords of  $J$  users, which will

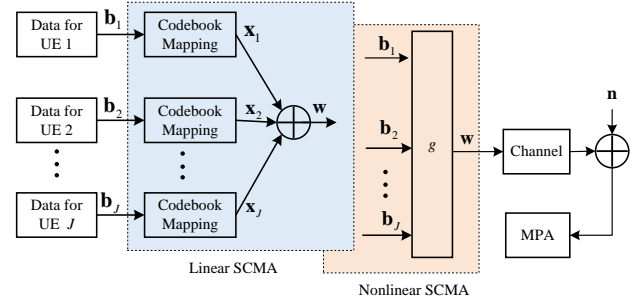


Fig. 2: Block diagram for the downlink linear and nonlinear SCMA systems.

constitute a superimposed constellation, denoted by  $\Phi_{M^J} \in \mathbb{C}^{K \times M^J}$ . Based on (5), the superimposed constellation can be obtained as

$$\Phi_{M^J} = \left\{ \sum_{j=1}^J \mathbf{x}_j \mid \forall \mathbf{x}_j \in \mathcal{X}_j, \forall j \right\}. \quad (6)$$

As a matter of fact, the mappings described by (4) and (5) are not necessary in downlink SCMA systems. Alternatively, the input message can be directly mapped to a vector  $\mathbf{w}$ . This leads to the definitions of the linear SCMA and NL-SCMA as follows:

*Definition 1:* If the transmitted codeword  $\mathbf{w}$  is obtained through (1) and (5), then it is called a linear SCMA system and the codebook  $\mathcal{X} = \{\mathcal{X}_1, \mathcal{X}_2, \dots, \mathcal{X}_J\}$  is said to be a LCB set. On the other hand, if the transmitted codeword  $\mathbf{w}$  is obtained by the following non-linear mapping rule:

$$g : \mathbb{B}^{\log_2 M \times J} \rightarrow \mathbf{w} \in \mathbb{C}^{K \times 1}, \quad \text{i.e., } \mathbf{w} = g(\mathbf{B}), \quad (7)$$

where  $\mathbf{B} = [\mathbf{b}_1, \mathbf{b}_2, \dots, \mathbf{b}_J]$ , then it is referred as a NL-SCMA system and the mapping  $g$  is said to be a NL-SCMA.

Fig. 2 shows an example of the linear SCMA and the proposed NL-SCMA systems. It is noted that the proposed NL-SCMA can serve as a general framework and subsume the existing linear SCMA systems as special cases. Denote  $\mathbf{h}_l \in \mathbb{C}^{K \times 1}$  as the channel vector from the base station to the  $l$ th UE. The received signal at the  $l$ th UE can be expressed as

$$\mathbf{y}_l = \begin{cases} \text{diag}(\mathbf{h}_l) \sum_{j=1}^J \mathbf{x}_j + \mathbf{n}_l & \text{Linear SCMA,} \\ \text{diag}(\mathbf{h}_l) g(\mathbf{B}) + \mathbf{n}_l & \text{Nonlinear SCMA,} \end{cases} \quad (8)$$

where  $\mathbf{n}_l$  denotes the noise vector at the  $l$ th UE that has  $\mathcal{CN}(0, N_0)$  entries. For simplicity, the subscript  $l$  in (8) is omitted whenever no ambiguity arises.

It is noted that the proposed NL-SCMA does not increase computational complexity compared to conventional SCMA systems. It requires the base station to store the superimposed constellation, which has  $K \times M^J$  complex-valued elements. In contrast, linear SCMA systems require the base station to store the codebooks of  $J$  users, which have  $JMK$  complex-valued elements.

### C. NL-SCMA Detection

Given the received signal  $\mathbf{y}$  and  $\mathbf{h}$ , the optimum maximum a posteriori probability detector finds the  $\hat{\mathbf{B}}$  that maximizes the

a posterior probability of the transmitted  $\mathbf{B}$ , i.e.,  $\Pr(\mathbf{B}|\mathbf{y})$ , by [29]

$$\tilde{\mathbf{B}} = \arg \max_{\mathbf{B} \in \mathbb{B}^{\log_2 M \times J}} \Pr(\mathbf{B}|\mathbf{y}, g). \quad (9)$$

According to Bayes' rule, we have

$$P(\mathbf{B}|\mathbf{y}, g) = \frac{\Pr(\mathbf{y}|\mathbf{B}, g)\Pr(\mathbf{B})}{\Pr(\mathbf{y})} \propto \Pr(\mathbf{y}|\mathbf{B}, g)\Pr(\mathbf{B}), \quad (10)$$

where  $P(\mathbf{B}) = \prod_{j=1}^J \Pr(\mathbf{b}_j)$  is the joint prior probability mass function. Under the Gaussian assumption of  $\mathbf{n}$ , we have

$$P(\mathbf{y}|\mathbf{B}, g) = \frac{1}{\sqrt{2\pi N_0}} \exp\left(-\frac{1}{2N_0} \|\mathbf{y} - \text{diag}(\mathbf{h})g(\mathbf{B})\|^2\right). \quad (11)$$

Solving problems (9)-(11) has exponential complexity. Thanks to the sparsity of the codewords, the solution of this problem can be approximated by an iterative decoding algorithm. Following the factor graph and the principles of the sum-product algorithm, the information transmitted from the  $k$ th RN ( $r_k$ ) to the  $j$ th UN ( $u_j$ ) can be expressed as [30]

$$\delta_{r_k \rightarrow u_j}^t(\mathbf{b}_j) = \sum_{\tilde{\mathbf{b}}_j \in \mathcal{B}} P(\mathbf{y}|\tilde{\mathbf{B}}, g) \prod_{l \in \xi_k \setminus \{j\}} \eta_{u_l \rightarrow r_k}^{t-1}, \quad (12)$$

where  $\tilde{\mathbf{B}} = [\tilde{\mathbf{b}}_1, \tilde{\mathbf{b}}_2, \dots, \tilde{\mathbf{b}}_J] \in \mathbb{B}^{\log_2 M \times J}$ ,  $\mathcal{B}$  denotes all possible  $\tilde{\mathbf{B}}$  matrices in which  $\mathbf{b}_j \neq \tilde{\mathbf{b}}_j$ , and  $\xi_k$  denotes the set of user indices which utilizes the  $k$ th resource. By contrast, the information conveyed from UN  $u_j$  to RN  $r_k$  is the product of the information collected from the UNs connected to RN  $r_k$  excluding UN  $u_j$ , which can be expressed as

$$\eta_{u_j \rightarrow r_k}^t = \prod_{m \in \zeta_j \setminus k} \delta_{r_m \rightarrow u_j}^{t-1}, \quad (13)$$

where  $\zeta_j$  is the set of nonzero's position in the  $j$ th column of  $\mathbf{F}_{K \times J}$ .

### III. SPARSE CODEBOOK DESIGN: DESIGN METRIC

In this section, we present the KPIs that are considered for designing advanced codebooks. To better understand the proposed codebook design principle, we recall briefly the state-of-the-art codebook design scheme.

#### A. SCMA Codebook Design KPIs

We start by introducing the MED and MPD in a linear SCMA system. The MED and MPD of an  $N$ -dimensional constellation  $\mathbf{A} = [\mathbf{a}_1, \mathbf{a}_2, \dots, \mathbf{a}_M] \in \mathbb{C}^{N \times M}$  are defined as [17], [22]

$$\text{MED}(\mathbf{A}) \triangleq \min_{\substack{1 \leq p, q \leq M, \\ p \neq q}} \|\mathbf{a}_p - \mathbf{a}_q\|, \quad (14)$$

and

$$\text{MPD}(\mathbf{A}) \triangleq \min_{p \neq q} \prod_{n \in \rho(\mathbf{a}_p, \mathbf{a}_q)} |a_{n,p} - a_{n,q}|^2, \quad (15)$$

respectively, where  $a_{n,p}$  denotes the  $n$ th entry of  $\mathbf{a}_p$  and  $\rho(\mathbf{a}_p, \mathbf{a}_q)$  denotes the set of indices in which  $a_{n,p} \neq a_{n,q}$ . The

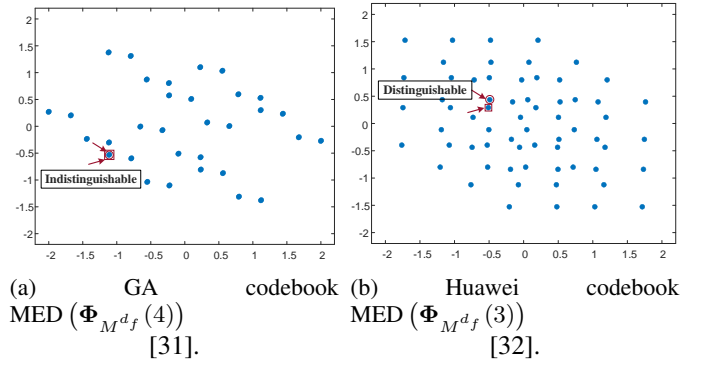


Fig. 3: Examples of the superimposed constellations.

MED of  $\Phi_{M^J}$  is obtain by calculating  $M^J (M^J - 1)$  mutual distances between  $M^J$  superimposed codewords<sup>1</sup>, i.e.,

$$\text{MED}(\Phi_{M^J}) \triangleq \min_{\substack{1 \leq p, q \leq M^J, \\ p \neq q}} \|\mathbf{w}_p - \mathbf{w}_q\|. \quad (16)$$

Analogous to the MED in linear SCMA systems, the MED of the superimposed codewords in the proposed NL-SCMA can be represented as

$$\text{MED}(\Phi_{M^J}) \triangleq \min_{\substack{\mathbf{B}, \tilde{\mathbf{B}}, \\ g(\mathbf{B}) \neq g(\tilde{\mathbf{B}})}} \|\mathbf{g}(\mathbf{B}) - \mathbf{g}(\tilde{\mathbf{B}})\|. \quad (17)$$

The MPD of the NL-SCMA will be introduced along with the NL-CB design in Section IV. In general, a large MED ( $\Phi_{M^J}$ ) leads to reliable detection in the Gaussian channels, whereas a large MPD ( $\mathcal{X}_j$ ) is preferred for robust transmissions in the Rayleigh fading channels [2].

#### B. The Top-Down Based Multi-Stage Codebook Design

It is worth mentioning that current codebook design approaches typically follow a top-down methodology by first constructing an MC, upon which certain phase rotations are applied to the MC to obtain codebooks for multiple users [15]–[21], [26]. These phase rotations aim to enhance the distance metric between superimposed codewords, thereby improving overall codebook performance. For  $K = 4, J = 6, N = 2$ , a Lattice based phase rotation matrix is widely considered, which takes the following expression:

$$\Theta_{4 \times 6} = \begin{bmatrix} 0 & e^{j\theta_3} & e^{j\theta_1} & 0 & e^{j\theta_2} & 0 \\ e^{j\theta_2} & 0 & e^{j\theta_3} & 0 & 0 & e^{j\theta_1} \\ 0 & e^{j\theta_2} & 0 & e^{j\theta_1} & 0 & e^{j\theta_3} \\ e^{j\theta_1} & 0 & 0 & e^{j\theta_2} & e^{j\theta_3} & 0 \end{bmatrix}, \quad (18)$$

where  $\theta_i \in [-\pi, \pi]$  is the phase rotation. The steps involved in the codebook design for AWGN or Rayleigh fading channels are summarized below.

**Step 1:** Select an one-dimensional basic constellation, denoted as  $\mathbf{a}_0 \in \mathbb{C}^{M \times 1}$ .

**Step 2:** The MC, defined as  $\mathbf{A}_{\text{MC}}$ , is obtained by the repetition and permutation of  $\mathbf{a}_0$ . Let  $\pi_n$  denote the permutation

<sup>1</sup>The metric of the MED and MPD of the MC, and the MED of the superimposed constellation are derived based on the PEP analysis of SCMA. We refer the readers to [2] and [16] for more details about the PEP formulation.

mapping of the  $n$ th dimension, then the  $N$ -dimensional MC can be obtained as

$$\mathbf{A}_{\text{MC}} = [\boldsymbol{\pi}_1(\mathbf{a}_0), \boldsymbol{\pi}_2(\mathbf{a}_0), \dots, \boldsymbol{\pi}_N(\mathbf{a}_0)]^T. \quad (19)$$

The permutation criteria are the MED ( $\mathbf{A}_{\text{MC}}$ ) and MPD ( $\mathbf{A}_{\text{MC}}$ ) for Gaussian and Rayleigh fading channels, respectively [2].

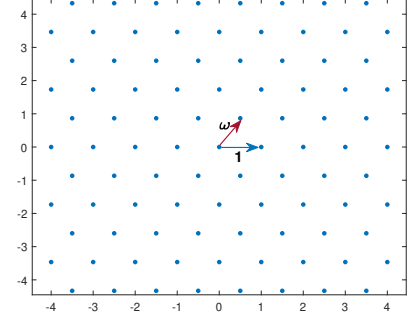
**Step 3:** The phase rotation angles are then applied to the  $\mathbf{A}_{\text{MC}}$  to design the codebook for different users. Specifically, the  $j$ th user's codebook is generated by  $\mathcal{X}_j = \mathbf{V}_j \boldsymbol{\Theta}_j \mathbf{A}_{\text{MC}}$ , where  $\boldsymbol{\Theta}_j$  is the phase operation matrix of  $j$ th user that determined by (18). Specifically,  $\boldsymbol{\Theta}_j$  can be constructed by applying the diagonal operation to the non-zero elements of the  $j$ th column in (18). For example, we have

$$\boldsymbol{\Theta}_1 = \begin{bmatrix} e^{j\theta_2} & 0 \\ 0 & e^{j\theta_1} \end{bmatrix}^T, \quad \boldsymbol{\Theta}_2 = \begin{bmatrix} e^{j\theta_3} & 0 \\ 0 & e^{j\theta_2} \end{bmatrix}^T. \quad (20)$$

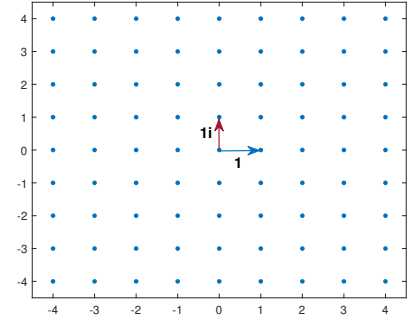
Denote  $\Phi_{M^{d_f}}(k)$  as the superimposed constellation at the  $k$ th subcarrier, and let  $d_f = |\xi_k|$ ,  $E_{\max}(\Phi_{M^{d_f}}(k))$ . The rotation angle should be optimized to improve distance profile of the superimposed codewords. Specifically, the optimum rotation angles  $\theta_i = 1, 2, \dots, d_f$  are determined by maximizing the MED ( $\Phi_{M^J}$ ), MED ( $\Phi_{M^{d_f}}(k)$ ), for Gaussian and Rayleigh fading channels, respectively [2], [16].

In downlink SCMA systems, the distance properties of the superimposed constellation, which are generally determined by the selection of an MC and rotation angles, have a significant impact on SCMA performance. On one hand, the top-down multi-stage codebook design is a sub-optimal approach, as it has been pointed out that the optimal way is to directly design the superimposed constellation. On the other hand, the search space for rotation angles and parameters in MC designs is generally large. Therefore, it is quite challenging to obtain an MC and rotation angles that simultaneously yield large MED ( $\Phi_{M^J}$ ), MED ( $\Phi_{M^{d_f}}(k)$ ), and MPD ( $\mathbf{A}_{\text{MC}}$ ). Fig. 4 shows an example of the  $\Phi_{M^{d_f}}(4)$  and  $\Phi_{M^{d_f}}(3)$  of the GA codebook [31] and Huawei codebook [32], respectively. The GA codebook is generated by first selecting a mother MC, followed by the application of phase rotation and power scaling, which are optimized using a genetic algorithm, to generate the codebook for different users. In Fig. 4(a), it is apparent that multiple constellation points overlap at the same position, rendering them indistinguishable in the fourth dimension. While these codewords can still be distinguished by other dimensions, this results in a sacrifice of diversity gain in the fourth dimension [16]. In this regard, the codebook  $\Phi_{M^{d_f}}(3)$  shown in Fig. 4(b) is more preferable than  $\Phi_{M^{d_f}}(4)$  depicted in Fig. 4(a) as all its elements are separated. However, Fig. 4(b) still experiences a small MED ( $\Phi_{M^{d_f}}(k)$ ). In this paper, a codebook is considered to be a ‘‘full diversity’’ codebook if its superimposed constellation satisfies  $\text{MED}(\Phi_{M^{d_f}}(k)) > 0$ ,  $1 \leq k \leq K$ . In addition to satisfying this condition, a large MED ( $\Phi_{M^{d_f}}(k)$ ) is also desirable for enhancing the diversity gain.

The objective of this work is to design an advanced class of NLCBs that exhibit low error rates in both Gaussian and Rayleigh fading channels, while simultaneously achieving desirable characteristics such as full diversity.



(a) Lattice constellation of the Eisenstein integers.



(b) Lattice constellation of the Gaussian integers.

Fig. 4: The employed lattice constellations.

#### IV. THE PROPOSED NLCB DESIGN

Different from the ‘‘top-down’’ based design principles, we follows a ‘‘down-top’’ based idea to construct the NL-SCMA codebooks based on the lattice constellation.

##### A. The Proposed Non-Linear SCMA Codebook

The first step in the proposed approach involves designing the superimposed constellation with desirable distance properties. Then, the objective is to determine the non-linear mapping between users' input bits and the superimposed constellation. The main steps involved in the codebook design for both AWGN and Rayleigh fading channels are briefly summarized follows:

- Designing an one-dimensional overlapped constellation  $\mathcal{S} \in \mathbb{C}^{M^{d_f} \times 1}$  with full diversity and large MED. Then,  $\mathcal{S}$  is utilized to design the superimposed constellation.
- For each RN, design the mapping between users' input bits to the overlapped constellation  $\mathcal{S}$ .
- Optimizing the overall mapping to attain large MED ( $\Phi_{M^J}$ ).

1) *Designing  $\mathcal{S}$  based on lattice code:* A lattice constellation is a regular, repeating arrangement of points in a multidimensional space. It can be thought of as a grid that extends infinitely in all directions within that space [33]. It has the advantages of good minimum MED, constellation volume, design flexibility, and shape gain. Hence, in this paper, we

consider lattice codes for the overlapped constellation design. The design process primarily consists of the following two steps.

**Step 1a): Generate the lattice constellation**

To begin with, we introduce the following definition:

*Definition 2:* A lattice is defined as the (infinite) set of points in an  $n$ -dimensional space given by all linear combinations with integer coefficients of a basis set of up to  $n$  linearly independent vectors [33]. Denote  $\Lambda \in \mathbb{C}^n$  as the  $n$ -dimensional complex-valued Lattice constellation, then  $\Lambda$  can be defined in terms of a generator matrix  $\mathbf{G} \in \mathbb{C}^{n \times 2n}$ , whose columns are the basis vectors:

$$\Lambda = \{\lambda = \mathbf{G}\mathbf{z} | \forall \mathbf{z} \in \mathbb{Z}^{2n}\}. \quad (21)$$

A lattice code is then defined by the finite set of lattice points within a certain region.

In this paper, we consider two lattice constellations, namely the Hexagonal constellation and the Gaussian lattice constellation [33]. The Hexagonal constellation can be generated based on the Eisenstein number, which takes the following expression

$$\nu = \exp\left(\frac{2\pi i}{3}\right), \quad (22)$$

where  $i = \sqrt{-1}$ . The above Eisenstein number is a root of  $x^2 + x + 1 = 0$ . For an one-dimensional complex lattice constellation,  $\mathbf{G}$  is a vector. As a matter of fact, by letting  $\mathbf{G} = [1, \nu]$ , (21) forms the one-dimensional hexagonal lattice in the complex domain [34]. In the theory of data packing, a hexagonal lattice is viewed as the best lattice for its largest packing distance.

Gaussian lattice constellation is also known as the Gaussian integers or the quadrature amplitude modulation (QAM) constellation. The one dimensional complex Gaussian integers can be generated by letting  $\mathbf{G} = [1, 1i]$ . Fig. 4 shows an example of the of hexagonal and Gaussian lattice constellations.

**Step 1b): Constellation partitioning**

A general method for constructing the overlapped constellation  $\mathcal{S}$  is to partition a subset constellation from a lattice constellation  $\Lambda$  that lies within some region  $\mathcal{R}$ . As such, the resultant  $\mathcal{S}$  is a lattice code [33]. An important characteristic in a Lattice constellation is the constellation shape gain, which is defined as follows:

*Definition 3:* The shape gain of a region  $\mathcal{R}$  is defined as [33]

$$\gamma_s(\mathcal{R}) = \frac{[V(\mathcal{R})]^{\frac{2}{n}}}{6P(\mathcal{R})}, \quad (23)$$

where  $V(\mathcal{R})$  is the volume of the region  $\mathcal{R}$ ,  $P(\mathcal{R})$  denotes the average energy of the constellation and  $n$  is the number of dimensions.

In general, a large shape gain is desirable for performance improvement [33]. Consequently, the shape gain is considered when in determining the partition regions. Overall, the principles in determining the partition regions are given as follows:

- The partition region should be chosen to enclose the desired number of signal points, i.e.,  $|\mathcal{S}| = M^{d_f}$ .
- A symmetric partition region is preferable as the partitioned constellations are more likely symmetric and own a zero mean.

- The partition region should be chosen to maximize the shape gain of the constellation, i.e.,  $\gamma_s(\mathcal{R})$ .

Considering the above partition rules, we employ two partition windows  $\mathcal{R}$ , namely the circular and rectangular windows. Fig. 5 shows an example the partitioned lattice codes based on the two windows for  $M = 4$  and  $d_f = 3$ . Compared to existing overlapped constellation, e.g., the overlapped constellations in Fig. 4, the proposed constellation owns a good geometric shape and large MED.

2) *Design the non-linear mapping:* Upon determining  $\mathcal{S}$ , the mapping between the incoming bits of  $d_f$  users to the  $\mathcal{S}$  at each subcarrier should be further designed. Let  $\mathbf{b} = [\mathbf{b}_1^T, \mathbf{b}_2^T, \dots, \mathbf{b}_{d_f}^T]^T$  be the incoming message vector of the  $d_f$  users with length of  $L = d_f \log_2(M)$ . Then, the mapping process can be implemented with a permutation matrix, which can be mathematically expressed as

$$\bar{\mathbf{b}} = \mathbf{P}\mathbf{b}, \quad (24)$$

where  $\mathbf{P} = \{p_{l,\nu}\} \in \mathbb{B}^{L \times L}$  is the bit mapping (permutation) matrix and  $p_{l,\nu} = 1$  denotes the  $l$ 'th bit in  $\mathbf{b}$  is mapped to the  $l$ 'th entry of  $\bar{\mathbf{b}}$ . Finally, the constellation point with a labeling of  $\bar{\mathbf{b}}$ , denoted by  $s_{\bar{\mathbf{b}}} \in \mathcal{S}$ , is selected for transmission. Moreover, since  $\mathbf{b}$  contains  $d_f$  users' bit message, we further denote the mapping from the  $i$ th position of  $\mathbf{b}$ , i.e.,  $\mathbf{b}_i$ , to  $\bar{\mathbf{b}}$  in (24) as

$$f_{\mathbf{P}}^i : \mathbf{b} \rightarrow \bar{\mathbf{b}}, 1 \leq i \leq d_f. \quad (25)$$

For example, for  $M = 4$  and

$$\mathbf{P} = \begin{bmatrix} 0 & 0 & 1 & 0 & 0 & 0 \\ 1 & 0 & 0 & 0 & 0 & 0 \\ 0 & 0 & 0 & 0 & 0 & 0 \\ 0 & 1 & 0 & 1 & 0 & 0 \\ 0 & 0 & 0 & 0 & 1 & 0 \\ 0 & 0 & 0 & 0 & 0 & 1 \end{bmatrix}, \quad (26)$$

$f_{\mathbf{P}}^1$  indicates that the incoming message bits, which are allocated to the first and second positions of  $\mathbf{b}$ , are mapped to the second and the fourth entries of  $\bar{\mathbf{b}}$ . Considering the factor graph in (2), the following mapping rule is employed to construct the NLCBs:

$$f_{\mathbf{F}_{4 \times 6}} = \begin{bmatrix} 0 & f_{\mathbf{P}}^3 & f_{\mathbf{P}}^1 & 0 & f_{\mathbf{P}}^2 & 0 \\ f_{\mathbf{P}}^2 & 0 & f_{\mathbf{P}}^3 & 0 & 0 & f_{\mathbf{P}}^1 \\ 0 & f_{\mathbf{P}}^2 & 0 & f_{\mathbf{P}}^1 & 0 & f_{\mathbf{P}}^3 \\ f_{\mathbf{P}}^1 & 0 & 0 & f_{\mathbf{P}}^2 & f_{\mathbf{P}}^3 & 0 \end{bmatrix}. \quad (27)$$

Based on (27), the first user employs the mapping principles  $f_{\mathbf{P}}^2$  and  $f_{\mathbf{P}}^1$  to map its input message to the second and fourth subcarrier, respectively, and the bits of  $j$ th user  $j = 2, \dots, J$  can be mapped in a similar way. For each RE, the mapping set is the same, leading to the same overlapped constellation  $\mathcal{S}$ .

3) *MED optimization:* In the proposed NL-SCMA, users' binary message are directly mapped to a superimposed code-word for transmission. Obviously, the MED of the superimposed constellation, i.e.,  $\text{MED}(\Phi_{M^J})$  depends on the  $f_{\mathbf{F}_{4 \times 6}}$  and the bit labeling of  $\mathcal{S}$ . In this regard, the mapping matrix  $\mathbf{P}$  and the labeling rule of  $\mathcal{S}$  can be constructed to achieve a large MED ( $\Phi_{M^J}$ ). A generalized approach is to conduct random search to find  $\mathbf{P}$  and labeling rule. **Algorithm 1** shows the proposed generalized MED optimization for the proposed



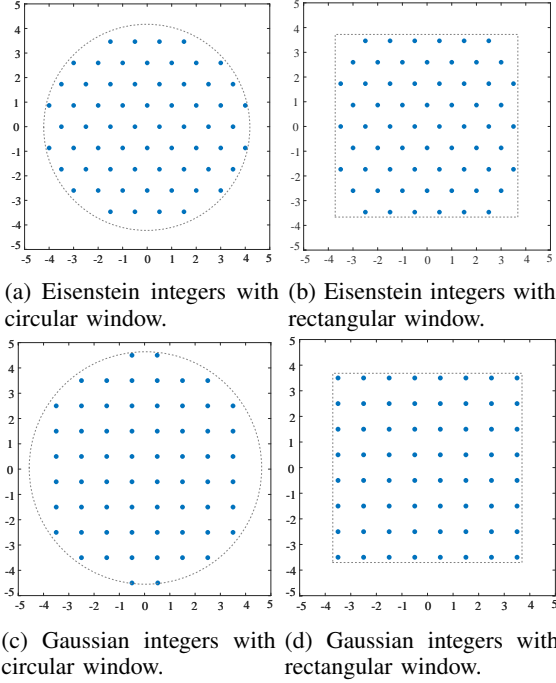


Fig. 5: Partitioned Lattice codes.

---

**Algorithm 1** Generalized NLCB Design.

---

**Require:** Nonlinear mapping  $f_{\mathbf{F}}$ , indicator matrix  $\mathbf{F}$ ,  $I_t$  and partition window  $\mathcal{R}$ .

**Step 1 :** Generate the lattice constellation.

2: **Step 2 :** Apply a partition window to the lattice constellation to obtain the overlapped constellation  $\mathcal{S}$ .

**Step 3 :** Maximizing  $\text{MED}(\Phi_{M^J})$ :

4: **for**  $i = 1 : I_t$  **do**

Randomly assign the bit mapping matrix and labeling.

6: Preserve the current results of  $\text{MED}(\Phi_{M^J})$ .

**end for**

8: Choose the best results of  $\mathbf{P}$  and labeling that has the maximum value of  $\text{MED}(\Phi_{M^J})$ .

---

NLCB. It is worth emphasizing here that the codebook design is an offline process, and once the codebook is obtained, it can be directly applied to a practical system.

In what follows we present a low complexity NLCB design which can avoid the random search. Specifically, an error-pattern inspired NLCB design is proposed to determine  $\mathbf{P}$  and the labeling rule for  $M = 4$  and  $d_f = 3$ . We begin with the analysis of the  $\text{MED}(\Phi_{M^J})$  of the proposed NL-SCMA.

Let us rewritten the instantaneous transmitted binary vector of  $J$  users as a matrix based on the indicator matrix as follows

$$\mathbf{B}_{4 \times 6} = \begin{bmatrix} \mathbf{0} & \mathbf{b}_2 & \mathbf{b}_3 & \mathbf{0} & \mathbf{b}_5 & \mathbf{0} \\ \tilde{\mathbf{b}}_1 & \mathbf{0} & \mathbf{b}_3 & \mathbf{0} & \mathbf{0} & \mathbf{b}_6 \\ \mathbf{0} & \mathbf{b}_2 & \mathbf{0} & \mathbf{b}_4 & \mathbf{0} & \mathbf{b}_6 \\ \tilde{\mathbf{b}}_1 & \mathbf{0} & \mathbf{0} & \mathbf{b}_4 & \mathbf{b}_5 & \mathbf{0} \end{bmatrix}. \quad (28)$$

For an instantaneous transmitted  $\mathbf{B}_{4 \times 6}$ , due to multiuser interference and additive white Gaussian noise, it is assumed to be erroneously decoded to another binary matrix at the receiver, denoted by  $\tilde{\mathbf{B}}_{4 \times 6}$ , where  $\tilde{\mathbf{B}}_{4 \times 6} \neq \mathbf{B}_{4 \times 6}$ . The error

patterns between  $\tilde{\mathbf{B}}_{4 \times 6}$  and  $\mathbf{B}_{4 \times 6}$  can be basically categorized into two patterns. In the case of the decoding errors occur with a single user only, the error pattern is called the ‘‘single-user error pattern (SUEP)’’; otherwise, it will be called the ‘‘multiple-user error patterns (MUEPs)’’ [7]. The following shows examples of a SUEP and MUEPs, respectively,

$$\tilde{\mathbf{B}}_{4 \times 6}^{(\text{SUEP})} = \begin{bmatrix} \mathbf{0} & \mathbf{b}_2 & \mathbf{b}_3 & \mathbf{0} & \mathbf{b}_5 & \mathbf{0} \\ \tilde{\mathbf{b}}_1 & \mathbf{0} & \mathbf{b}_3 & \mathbf{0} & \mathbf{0} & \mathbf{b}_6 \\ \mathbf{0} & \mathbf{b}_2 & \mathbf{0} & \mathbf{b}_4 & \mathbf{0} & \mathbf{b}_6 \\ \tilde{\mathbf{b}}_1 & \mathbf{0} & \mathbf{0} & \mathbf{b}_4 & \mathbf{b}_5 & \mathbf{0} \end{bmatrix}, \quad (29)$$

and

$$\tilde{\mathbf{B}}_{4 \times 6}^{(\text{MUEPs})} = \begin{bmatrix} \mathbf{0} & \mathbf{b}_2 & \mathbf{b}_3 & \mathbf{0} & \tilde{\mathbf{b}}_5 & \mathbf{0} \\ \tilde{\mathbf{b}}_1 & \mathbf{0} & \mathbf{b}_3 & \mathbf{0} & \mathbf{0} & \mathbf{b}_6 \\ \mathbf{0} & \mathbf{b}_2 & \mathbf{0} & \mathbf{b}_4 & \mathbf{0} & \mathbf{b}_6 \\ \tilde{\mathbf{b}}_1 & \mathbf{0} & \mathbf{0} & \mathbf{b}_4 & \tilde{\mathbf{b}}_5 & \mathbf{0} \end{bmatrix}. \quad (30)$$

It is noted that the error pattern in Gaussian channels directly relates to the MED features of the superimposed constellation. In high SNR region, if the MED ( $\Phi_{M^J}$ ) is observed within a single user only, then the SUEP dominates the error rate performance of the codebook, otherwise, the MUEPs dominates. To proceed, let us reformulate MED ( $\Phi_{M^J}$ ) as

$$\text{MED}(\Phi_{M^J}) = \min \left\{ \text{MED}^{\text{SUEP}}(\Phi_{M^J}), \text{MED}^{\text{MUEPs}}(\Phi_{M^J}) \right\}, \quad (31)$$

where  $\text{MED}^{\text{SUEP}}(\Phi_{M^J})$  and  $\text{MED}^{\text{MUEPs}}(\Phi_{M^J})$  denote the MED between the SUEP and MUEPs, respectively. In the existing linear SCMA codebooks, e.g., [14], [16], [18]–[21], [26], the following generally holds

$$\text{MED}^{\text{SUEP}}(\Phi_{M^J}) = \min_{1 \leq j \leq J} \text{MED}(\mathcal{X}_j) > \text{MED}^{\text{MUEPs}}(\Phi_{M^J}), \quad (32)$$

which indicates the MUEPs dominate the error rate performance. For example, the codebooks in [16] and [32] have the same  $\text{MED}^{\text{SUEP}}(\Phi_{M^J}) = 1.4$ , whereas the  $\text{MED}^{\text{MUEPs}}(\Phi_{M^J})$  are given by 1.07 and 0.56, respectively. Therefore, numeral efforts were paid to maximize the  $\text{MED}^{\text{MUEPs}}(\Phi_{M^J})$ . On the other hand, we show that the proposed NL-SCMA codebook owns a large lower bound of  $\text{MED}^{\text{MUEPs}}(\Phi_{M^J})$ . Let us define the element-wise distance at the  $k$ th entry between the transmitted vector  $\mathbf{w}$  and decoded vector  $\tilde{\mathbf{w}}$  as  $\tau_{\mathbf{w} \rightarrow \tilde{\mathbf{w}}}(k)$ . For for MUEPs in (30), we have

$$\tau_{\mathbf{w} \rightarrow \tilde{\mathbf{w}}}(k) \geq \text{MED}(\mathcal{S}), k \in \{1, 2, 4\}. \quad (33)$$

Obviously,  $\text{MED}^{\text{MUEPs}}(\Phi_{M^J})$  is lower bounded by

$$\text{MED}^{\text{MUEPs}}(\Phi_{M^J}) \geq (d_v + 1) \text{MED}(\mathcal{S}). \quad (34)$$

Since the designed Lattice code owns a large  $\text{MED}(\mathcal{S})$ , the  $\text{MED}^{\text{MUEPs}}(\Phi_{M^J})$  can be guaranteed to be a large value. Hence, the remaining problem is to find a labeling and mapping rule that achieves a large  $\text{MED}^{\text{SUEP}}(\Phi_{M^J})$ .

Recall (24), for  $M = 4$  and  $d_f = 3$ ,  $\tilde{\mathbf{b}}$  can be expressed as  $\tilde{\mathbf{b}} = [\tilde{\mathbf{b}}_H^T, \tilde{\mathbf{b}}_M^T, \tilde{\mathbf{b}}_L^T]^T$ , where  $\tilde{\mathbf{b}}_H \in \mathbb{B}^{\log_2(M) \times 1}$ ,  $\tilde{\mathbf{b}}_M \in \mathbb{B}^{\log_2(M) \times 1}$  and  $\tilde{\mathbf{b}}_L \in \mathbb{B}^{\log_2(M) \times 1}$  denote the highest, medium and least significant bit layers, respectively. Then, the MED of  $\tilde{\mathbf{b}}_H$  can be expressed as

$$d_{\min, \tilde{\mathbf{b}}_H}^{\mathcal{S}} = \min_{\substack{\tilde{\mathbf{b}}_H' \neq \tilde{\mathbf{b}}_H \\ \tilde{\mathbf{b}}_M' = \tilde{\mathbf{b}}_M, \tilde{\mathbf{b}}_L' = \tilde{\mathbf{b}}_L}} |s_{\tilde{\mathbf{b}}} - s_{\tilde{\mathbf{b}}'}|^2. \quad (35)$$

---

**Algorithm 2** Error Pattern-Inspired NLCB Design.
 

---

- Initialize:**  $\mathbf{P} = \mathbf{I}_L$ .
- 2: **Step 1** : The constellations are divided equally into  $M$  groups based on their quadrant. Then, each group is labeled with the same labeling at the HSBs.
- for**  $m$ th group **do**
- 4:   **for**  $i = 1 : I_t$  **do**  
       Label the HSBs and LSBs randomly.
- 6:    Preserve the current labeling if  $d_{\min, \tilde{\mathbf{b}}_H}^{\mathcal{S}} \geq d_{\min, \tilde{\mathbf{b}}_M}^{\mathcal{S}} \geq \gamma_{\text{th}}$ .
- end for**
- 8: **end for**  
 Construct the NLCB based on the bit layer assignment matrix in (39).
- 

Similarly, we can obtain the MED of  $\tilde{\mathbf{b}}_M$  and  $\tilde{\mathbf{b}}_L$ , which are denoted as  $d_{\min, \tilde{\mathbf{b}}_M}^{\mathcal{S}}$  and  $d_{\min, \tilde{\mathbf{b}}_L}^{\mathcal{S}}$ , respectively.

In the proposed error pattern-inspired codebook design, priority is assigned to the highest and medium significant bit layers. Our objective is to determine a labeling rule that maximizes  $d_{\min, \tilde{\mathbf{b}}_H}^{\mathcal{S}}$  and  $d_{\min, \tilde{\mathbf{b}}_M}^{\mathcal{S}}$ . Specifically, the constellation is first divided into  $M$  groups, denoted as  $\mathcal{S}(1), \mathcal{S}(2), \dots, \mathcal{S}(M)$ , respectively, where each group consists of  $M^{d_f-1}$  elements. In particular, it is preferable to assign the elements within the same quadrant to the same group. Then, all of the signals in each group are labeled with the same bit values at the highest significant bit layer, as such, we can obtain more degree of freedoms for improving  $d_{\min, \tilde{\mathbf{b}}_M}^{\mathcal{S}}$  due to the  $M$  groups are well separated. Denote  $d_{\min, \tilde{\mathbf{b}}_M}^{\mathcal{S}(m)}$  by the MED of the medium significant bit layers in the  $m$ th group, which takes the following expression

$$d_{\min, \tilde{\mathbf{b}}_M}^{\mathcal{S}(m)} = \min_{\substack{s_{\tilde{\mathbf{b}}'} \in \mathcal{S}(m), \\ \tilde{\mathbf{b}}'_M \neq \tilde{\mathbf{b}}_M, \tilde{\mathbf{b}}'_L = \tilde{\mathbf{b}}_L}} |s_{\tilde{\mathbf{b}}} - s_{\tilde{\mathbf{b}}'}|^2. \quad (36)$$

Subsequently, the labeling of the medium significant bit layers at each layer are carried out by maximizing  $d_{\min, \tilde{\mathbf{b}}_M}^{\mathcal{S}(m)}$  while maintaining  $d_{\min, \tilde{\mathbf{b}}_H}^{\mathcal{S}}$  larger than a threshold  $\gamma_{\text{th}}$ . Then  $d_{\min, \tilde{\mathbf{b}}_M}^{\mathcal{S}}$  can be expressed as

$$d_{\min, \tilde{\mathbf{b}}_M}^{\mathcal{S}} = \min_{1 \leq m \leq M} d_{\min, \tilde{\mathbf{b}}_M}^{\mathcal{S}(m)}. \quad (37)$$

The detailed steps of the proposed error pattern-inspired NLCB design are summarized in **Algorithm 2**. Since the priority is assigned to  $d_{\min, \tilde{\mathbf{b}}_H}^{\mathcal{S}}$  and  $d_{\min, \tilde{\mathbf{b}}_M}^{\mathcal{S}}$ , we have

$$d_{\min, \tilde{\mathbf{b}}_H}^{\mathcal{S}} \geq d_{\min, \tilde{\mathbf{b}}_M}^{\mathcal{S}} \geq d_{\min, \tilde{\mathbf{b}}_L}^{\mathcal{S}} \geq \text{MED}(\mathcal{S}). \quad (38)$$

To improve  $\text{MED}^{\text{SUEP}}(\Phi_{M^J})$  and achieve fairness between  $J$  users, the following mapping rule is considered:

$$\mathbf{f}_{\mathbf{F}^{4 \times 6}} = \begin{bmatrix} 0 & f_{\mathbf{P}}^1 & f_{\mathbf{P}}^2 & 0 & f_{\mathbf{P}}^3 & 0 \\ f_{\mathbf{P}}^3 & 0 & f_{\mathbf{P}}^2 & 0 & 0 & f_{\mathbf{P}}^1 \\ 0 & f_{\mathbf{P}}^3 & 0 & f_{\mathbf{P}}^2 & 0 & f_{\mathbf{P}}^1 \\ f_{\mathbf{P}}^1 & 0 & 0 & f_{\mathbf{P}}^2 & f_{\mathbf{P}}^3 & 0 \end{bmatrix}, \quad (39)$$

where  $\mathbf{P} = \mathbf{I}_L$ ,  $f_{\mathbf{P}}^1$ ,  $f_{\mathbf{P}}^2$ , and  $f_{\mathbf{P}}^3$  denote the mapping of input message to the highest, medium and least significant bit layers, respectively. In (39), the user maps its binary bits to the least

significant bit layers of  $\mathcal{S}$  at one subcarrier will assign its bits to the highest significant bit layers of  $\mathcal{S}$  at another subcarrier. As such,  $\text{MED}^{\text{SUEP}}(\Phi_{M^J})$  can be improved. Based on (39), the  $\text{MED}^{\text{SUEP}}(\Phi_{M^J})$  is given by

$$\text{MED}^{\text{SUEP}}(\Phi_{M^J}) = \min \left\{ d_{\min, \tilde{\mathbf{b}}_H}^{\mathcal{S}} + d_{\min, \tilde{\mathbf{b}}_L}^{\mathcal{S}}, 2d_{\min, \tilde{\mathbf{b}}_M}^{\mathcal{S}} \right\}. \quad (40)$$

Similarly, the MPD of the proposed NLCB is given by

$$\text{MPD}(\Phi_{M^J}) = \min \left\{ d_{\min, \tilde{\mathbf{b}}_H}^{\mathcal{S}} d_{\min, \tilde{\mathbf{b}}_L}^{\mathcal{S}}, (d_{\min, \tilde{\mathbf{b}}_M}^{\mathcal{S}})^2 \right\}. \quad (41)$$

To sum up, we have proposed a generalized architecture of designing the NLCBs based on lattice codes. Then an error pattern-inspired NLCB design is further proposed to simply the bit labeling and mapping design.

## V. NUMERICAL RESULTS

In this section, we conduct numerical simulations to evaluate the proposed NLCBs. The proposed NLCBs based on Lattice codes shown in Figs. 5(a)-(d) are named as NLCB1, NLCB2, NLCB3, NLCB4, respectively. For comparison, we consider the GAM codebook [17], Huawei codebook [32], and Chen's codebook [16]<sup>2</sup>. Specifically, the codebooks designed for Gaussian and Rayleigh fading channels in [16] are named as Chen-G and Chen-R, respectively. Moreover, we consider a Rician fading channels, i.e.,  $h_k \sim \mathcal{CN} \left( \sqrt{\frac{\kappa}{1+\kappa}}, \sqrt{\frac{1}{1+\kappa}} \right)$  with  $\kappa$  represents the ratio of average power in the LoS path over that in the scattered component. For  $\kappa = 0$  and  $\kappa \rightarrow \infty$ , the Rician fading channels are the Gaussian and Rayleigh fading channels, respectively.

### A. KPIs comparison

Table I compares the KPIs of various codebooks. One can see that the proposed codebooks own large MED ( $\Phi_{M^{d_f}}(k)$ ) than other codebooks. In particular, the proposed NLCB1 achieves the largest MED ( $\Phi_{M^{d_f}}(k)$ ). Moreover, the proposed NLCBs with circular window own slightly larger value of MED ( $\Phi_{M^{d_f}}(k)$ ) than that of the codebook obtained with a rectangular window. In addition, the proposed NLCB4 codebooks own the same MED with the Chen-G codebook. However, the proposed NLCB4 codebooks can attain better KPI performances in terms of MED ( $\Phi_{M^{d_f}}(k)$ ), MPD and diversity than the Chen-G codebook.

### B. Uncoded BER performance

Fig. 6 and Fig. 7 compare the BER performance of various codebooks in an uncoded system. Specifically, the proposed NLCB1 and NLCB4 are employed, where the MPA iterations is  $I = 7$ . The Chen-G is considered for Gaussian channels, whereas the Chen-R is employed in Fig. 7. As can be seen from the figures, the proposed codebooks achieve promising BER performance in Gaussian, Rayleigh and Rician ( $\kappa = 7$ )

<sup>2</sup>It was shown in [21] that the Huawei codebook and GAM codebook outperform many state-of-the-art codebooks in terms of the coded BER performance. Additionally, the Chen codebook exhibits promising uncoded BER performance [16]. Consequently, for demonstrate the superiority of the proposed codebooks, we consider the Huawei codebook, GAM codebook, and Chen codebook as the primary benchmark codebooks for the BER comparison.



TABLE I: Comparison of the KPIs of different codebooks. ‘‘Gau.’’ and ‘‘Ray.’’ denote the Gaussian and Rayleigh fading channels, respectively.

Codebook	Target Channels	MED ( $\Phi_{M^J}$ )	MED ( $\Phi_{M^{d_f}}(k)$ )	MPD	Shape gain, $\gamma_s$ ( $\mathcal{R}$ )
Prop. NLCB1	Gau.& Ray.	0.94	0.413	0.61	5.90
Prop. NLCB2	Gau.& Ray.	0.92	0.410	0.60	4.65
Prop. NLCB3	Gau.& Ray.	1.02	0.383	0.58	6.21
Prop. NLCB4	Gau.& Ray.	1.07	0.378	0.58	5.90
Huawei [32]	Gau.& Ray.	0.56	0.146	0.85	-
GAM [17]	Gau.& Ray.	0.56	0.000	0.69	-
Chen-G	Gau.	1.07	0.016	0.78	-
Chen-R	Ray.	0.84	0.199	1.0	-

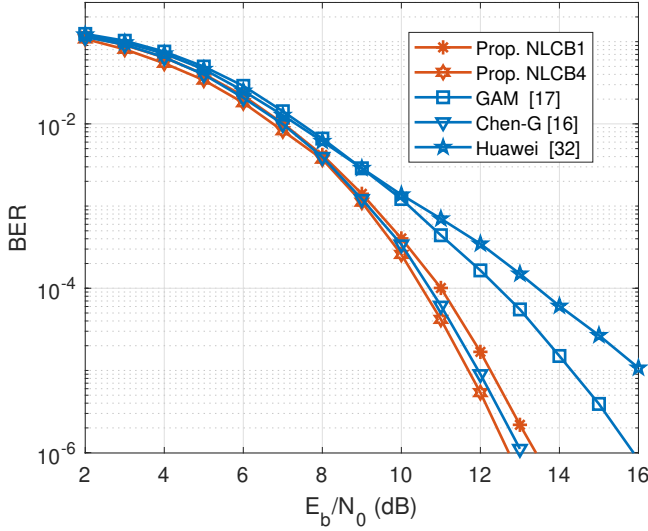


Fig. 6: BER performance of various codebooks over Gaussian channels.

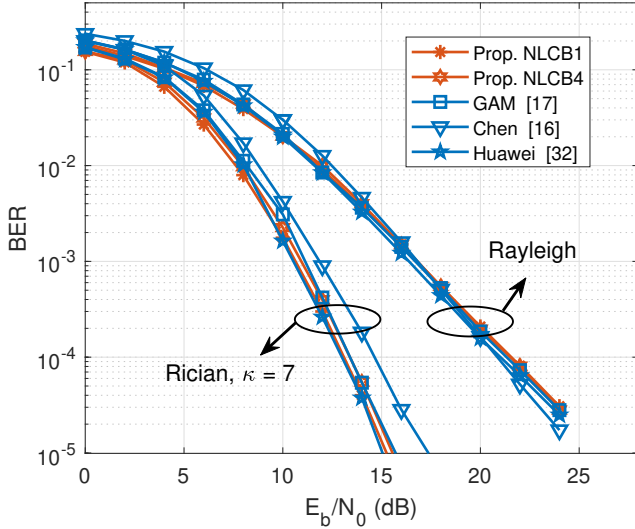


Fig. 7: BER performance of various codebooks over Rician fading channels ( $\kappa = 0$  and  $\kappa = 7$ ).

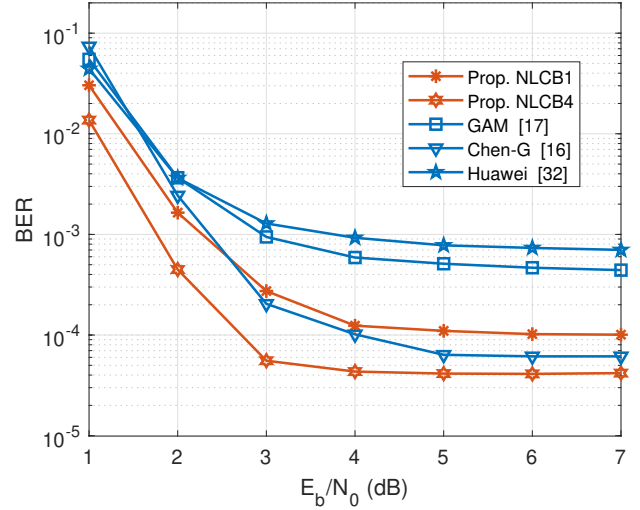


Fig. 8: BER performance v.s. number of MPA iterations

fading channels. In Gaussian channels, the proposed NLCB1 achieves about 4 dB gain over the Huawei codebook at the BER of  $10^{-5}$ . Although the MED of the proposed NLCB1 is the same with Chen codebook, the proposed NLCB1 still outperform the Chen codebook slightly. The main reason is that for the proposed codebook, we have  $\text{MED}(\Phi_{M^J}) = \text{MED}^{\text{SUEP}}(\Phi_{M^J})$ , whereas  $\text{MED}(\Phi_{M^J}) = \text{MED}^{\text{MU}}(\Phi_{M^J})$  holds for the Chen-G codebook. Namely, the SUEP and MUEPs dominant the BER performance of the proposed codebooks and the Chen-G codebook, respectively. It is evident that the SUEP has smaller Hamming distance than that of MUEPs. Hence, the proposed NLCB1 can attain better BER performance.

Observed from Fig. 7, all the codebooks achieve a similar BER performance at the medium SNRs over Rayleigh fading channels. It is worth mentioning that the proposed codebooks achieve better performance than the benchmark codebooks in the low SNR regions, whereas the Chen-R codebook performs the best at the high SNR regions in Rayleigh fading channels. This is reasonable, as lower bounding the MED of all superimposed signal vectors helps improve performance in the low-SNR region, while improving the MPD is beneficial for enhancing error rate performance in the high-SNR region for downlink Rayleigh fading channels. The proposed codebooks achieve a similar BER performance with GAM and Huawei

TABLE II: Simulation Parameters

Parameters	Values
Transmission	Downlink
Channel model	Gaussian and Rayleigh fading channels
SCMA setting	$\lambda = 150\%$ , $K = 4$ , $J = 6$
Channel coding	5G NR LDPC codes with code length = 512, and rate = 0.75 (Fig. 9) and 0.50 (Fig. 10).
Codebooks	NLCB1, NLCB4, GAM, Chen-G, Chen-R, and Huawei codebooks
Receiver	Turbo-MPA: 3 MPA iterations, 10 LDPC iterations, and 4 outer iterations.

codebook in the medium-to-high SNR regions in the Rician fading channels of  $\kappa = 7$ . Similar to their performance in Rayleigh fading channels, the proposed codebooks outperform other codebooks in low SNR regions.

Fig. 8 shows the BER performance with different number of MPA iterations of various codebooks in Gaussian channels. As can be seen from the figure, similar to the beach-marking codebooks, the proposed codebooks also require about 4 MPA iterations to converge.

### C. Coded BER performance

In this subsection, we evaluate the performance of different codebooks in a bit-interleaved coded modulation (BICM) system. Specifically, the iterative Turbo receiver in [7] is employed. At the receiver side, Turbo decoding is carried out between MPA decoder and channel decoder by iteratively exchanging soft information in the form of log-likelihood ratio (LLR) including *a priori* LLR and *a posterior* LLR (extrinsic).

Figs. 9-11 compare the BER performance of the LDPC coded BICM systems. The detailed simulation parameters are summarized in Table II. As can be seen from Fig. 9, the proposed NLCB4 achieves about 1 dB gain over the Chen-G codebook in Gaussian channels at BER of  $10^{-4}$ , whereas the proposed NLCB1 outperforms the Huawei and GAM codebook by 1.5 dB over Rayleigh fading channels. It should be noted that the proposed codebooks can performance well in both Gaussian and Rayleigh fading channels, however, this may not hold for the benchmark codebooks. Another observation is that a codebook that achieves better BER performance in an uncoded system may not outperform in a BICM system, and vice versa, which is also pointed out in our previous work [35].

We further compare the coded BER performance with rate of 0.5, which is shown in Fig. 10. The gains between the proposed codebooks and the benchmark codebooks are smaller compared to that of rate of 0.75 in Fig. 9. However, the proposed NLCB1 can still outperform the Huawei and GAM codebook by 1 dB over Rayleigh fading channels at the BER of  $10^{-4}$ . In addition, the proposed NLCB4 can achieve about 0.5 dB gain over the Chen codebook in Gaussian channels at the BER of  $10^{-4}$ . In addition, Fig. 11 shows the coded BER performance of different codebooks for Rician fading channels with  $\kappa = 7$ . The proposed NLCB1 still exhibits the best BER performance in Rician fading channels. It is also interesting

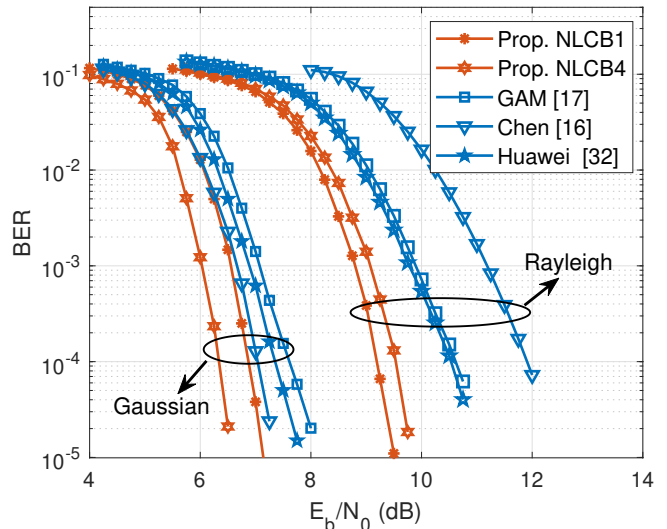


Fig. 9: LDPC coded BER performance of various codebooks with rate of 0.75.

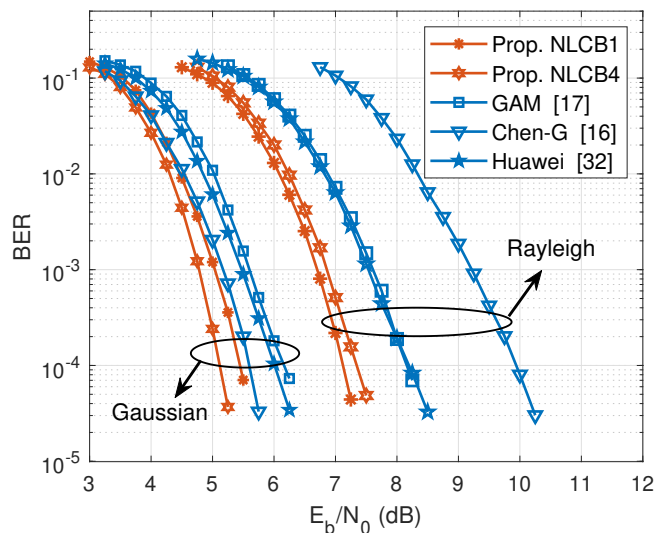


Fig. 10: LDPC coded BER performance of various codebooks with rate of 0.5.

to observe that, although the Chen-G codebook is designed for Gaussian channels, it significantly outperforms the GAM and Huawei codebooks in Rician fading channels. Overall, the benefits of the proposed codebooks are more prominent in a coded system.

## VI. CONCLUSION

In this paper, we have proposed a novel class of NL-SCMA codebooks. Different from the existing SCMA schemes, where the incoming bits are first mapped to a sparse codeword and then superimposed for transmission, the proposed NL-SCMA directly maps the incoming bits to a superimposed codeword. Despite the widely employed design KPIs in previous SCMA works, such as MED and MPD, we have also introduced the

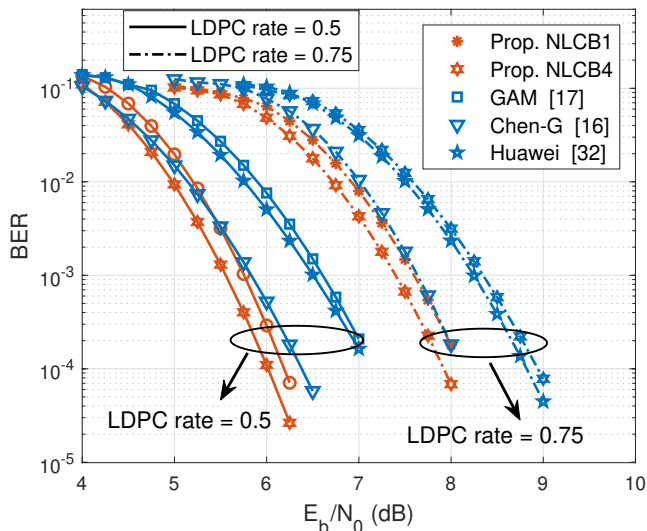


Fig. 11: LDPC coded BER performance of various codebooks with  $\kappa = 7$ .

diversity and shape gain of a codebook as the design KPIs. For efficient codebook design, different from the existing “top-down” based design principles, we have proposed a “down-top” based scheme to construct the NLCBs. Specifically, we have adopted the Lattice codes as the superimposed constellation by partitioning a Lattice constellation. As such, large shape gain can be guaranteed due to the inherent superiority of the Lattice constellations. Upon determining the one dimensional Lattice code, a generalized NLCB design has been proposed to design the mapping between the input message and superimposed constellation by improving the MED ( $\Phi_{M^J}$ ). In addition, by carefully analyzing the error patterns in the NL-SCMA systems, an error pattern-inspired NLCB design has been proposed to improve the MED ( $\Phi_{M^J}$ ) while can significantly reduce the computational complexity during optimization. Numerical results shown that the proposed NLCBs can simultaneously achieve promising BER performance over both Gaussian and Rayleigh fading channels in uncoded and coded systems, whistling achieving full diversity and large shape gain. In particular, significant BER gain has been observed of the proposed codebooks for the BICM system.

#### APPENDIX A THE PROPOSED CODEBOOKS

The proposed  $\mathcal{S}$  of NLCB1 is shown in Fig. 12. For the simplify of presentation, the bit labeling of “00”, “01”, “10”, “11” in each bit layer of  $\tilde{\mathbf{b}}$  are represented by the decimal numbers “0”, “1”, “2”, “3”, respectively. For example, the constellation point labelled with  $\tilde{\mathbf{b}} = [0, 0, 0, 1, 1, 0]$ , i.e.,  $\tilde{\mathbf{b}}_H = [0, 0]$ ,  $\tilde{\mathbf{b}}_M = [0, 1]$ ,  $\tilde{\mathbf{b}}_L = [1, 0]$ , is represented by “012”. NLCB1 and NLCB4 can be constructed based on Fig. 12 with the mapping defined in (39) and  $\mathbf{W} = \text{diag}(\mathbf{I}_J)$ .

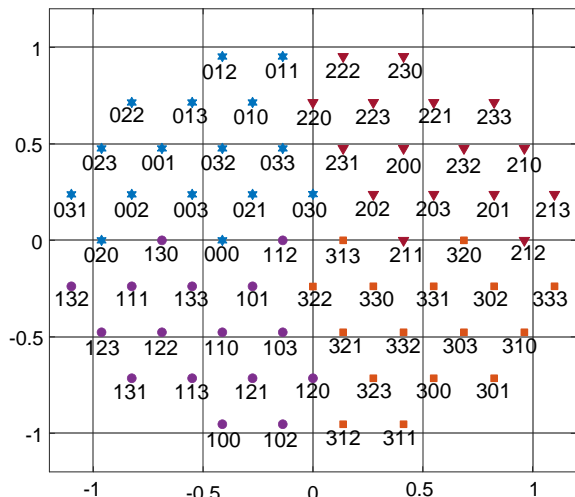


Fig. 12: The overlapped constellation  $\mathcal{S}$  of NLCB1.

#### REFERENCES

- [1] Y. Liu, S. Zhang, X. Mu, Z. Ding, R. Schober, N. Al-Dhahir, E. Hossain, and X. Shen, “Evolution of NOMA toward next generation multiple access (NGMA) for 6G,” *IEEE J. Sel. Areas Commun.*, vol. 40, no. 4, pp. 1037–1071, 2022.
- [2] Q. Luo, Z. Liu, G. Chen, P. Xiao, Y. Ma, and A. Maaref, “A design of low-projection SCMA codebooks for ultra-low decoding complexity in downlink IoT networks,” *IEEE Trans. Wireless Commun.*, 2023.
- [3] S. M. R. Islam, N. Avazov, O. A. Dobre, and K.-s. Kwak, “Power-domain non-orthogonal multiple access (NOMA) in 5G systems: Potentials and challenges,” *IEEE Communications Surveys & Tutorials*, vol. 19, no. 2, pp. 721–742, 2017.
- [4] Z. Yuan, G. Yu, W. Li, Y. Yuan, X. Wang, and J. Xu, “Multi-user shared access for Internet of Things,” in *IEEE VTC Spring*, 2016, pp. 1–5.
- [5] S. Chen, B. Ren, Q. Gao, S. Kang, S. Sun, and K. Niu, “Pattern division multiple access—a novel nonorthogonal multiple access for fifth-generation radio networks,” *IEEE Trans. Veh. Technol.*, vol. 66, no. 4, pp. 3185–3196, 2017.
- [6] S. Hu, B. Yu, C. Qian, Y. Xiao, Q. Xiong, C. Sun, and Y. Gao, “Nonorthogonal interleave-grid multiple access scheme for industrial Internet of things in 5G network,” *IEEE Transactions on Industrial Informatics*, vol. 14, no. 12, pp. 5436–5446, 2018.
- [7] Z. Liu and L.-L. Yang, “Sparse or dense: A comparative study of code-domain NOMA systems,” *IEEE Trans. Wireless Commun.*, vol. 20, no. 8, pp. 4768–4780, Aug. 2021.
- [8] Q. Luo, P. Gao, Z. Liu, L. Xiao, Z. Mheich, P. Xiao, and A. Maaref, “An error rate comparison of power domain non-orthogonal multiple access and sparse code multiple access,” *IEEE Open J. Commun. Society*, vol. 2, pp. 500–511, 2021.
- [9] H. Cheng, C. Zhang, Y. Huang, and L. Yang, “Efficient message passing receivers for downlink MIMO-SCMA systems,” *IEEE Trans. Veh. Tech.*, vol. 71, no. 5, pp. 5073–5086, 2022.
- [10] L. Chai, Z. Liu, P. Xiao, A. Maaref, and L. Bai, “An improved EPA-based receiver design for uplink LDPC coded SCMA system,” *IEEE Wireless Commun. Lett.*, vol. 11, no. 5, pp. 947–951, 2022.
- [11] Y.-M. Chen, Y.-C. Hsu, M.-C. Wu, R. Singh, and Y.-C. Chang, “On near-optimal codebook and receiver designs for MIMO-SCMA schemes,” *IEEE Trans. Wireless Commun.*, vol. 21, no. 12, pp. 10724–10738, 2022.
- [12] W. Yuan, N. Wu, Q. Guo, Y. Li, C. Xing, and J. Kuang, “Iterative receivers for downlink MIMO-SCMA: Message passing and distributed cooperative detection,” *IEEE Trans. Wireless Commun.*, vol. 17, no. 5, pp. 3444–3458, 2018.
- [13] R. Hoshyari, F. P. Wathan, and R. Tafazolli, “Novel low-density signature for synchronous CDMA systems over AWGN channel,” *IEEE Trans. Signal Processing*, vol. 56, no. 4, pp. 1616–1626, 2008.
- [14] C. Huang, B. Su, T. Lin, and Y. Huang, “Downlink SCMA codebook design with low error rate by maximizing minimum euclidean distance of superimposed codewords,” *IEEE Trans. Vehi. Tech.*, vol. 71, no. 5, pp. 5231–5245, 2022.

- [15] D. Cai, P. Fan, X. Lei, Y. Liu, and D. Chen, "Multi-dimensional SCMA codebook design based on constellation rotation and interleaving," in *2016 IEEE 83rd VTC Spring*, 2016, pp. 1–5.
- [16] Y.-M. Chen and J.-W. Chen, "On the design of near-optimal sparse code multiple access codebooks," *IEEE Trans. Commun.*, vol. 68, no. 5, pp. 2950–2962, Feb. 2020.
- [17] Z. Mheich, L. Wen, P. Xiao, and A. Maaref, "Design of SCMA codebooks based on golden angle modulation," *IEEE Trans. Veh. Technol.*, vol. 68, no. 2, pp. 1501–1509, Dec. 2018.
- [18] H. Yan, H. Zhao, Z. Lv, and H. Yang, "A top-down SCMA codebook design scheme based on lattice theory," in *Proc. IEEE 27th Int.Symp. Pers., Indoor, Mobile Radio Commun. (PIMRC)*, Valencia, Spain, Dec. 2016, pp. 1–5.
- [19] K. Xiao, B. Xia, Z. Chen, B. Xiao, D. Chen, and S. Ma, "On capacity-based codebook design and advanced decoding for sparse code multiple access systems," *IEEE Trans. Wireless Commun.*, vol. 17, no. 6, pp. 3834–3849, June 2018.
- [20] V. Vikas, A. Rajesh, K. Deka, and S. Sharma, "A comprehensive technique to design SCMA codebooks," *IEEE Commun. Lett.*, vol. 26, no. 8, pp. 1735–1739, 2022.
- [21] X. Zhang, D. Zhang, L. Yang, G. Han, H.-H. Chen, and D. Zhang, "SCMA codebook design based on uniquely decomposable constellation groups," *IEEE Trans. Wireless Commun.*, vol. 20, no. 8, pp. 4828–4842, Mar. 2021.
- [22] X. Li, Z. Gao, Y. Gui, Z. Liu, P. Xiao, and L. Yu, "Design of power-imbalanced SCMA codebook," *IEEE Tran. Veh. Tech.*, vol. 71, no. 2, pp. 2140–2145, Feb. 2022.
- [23] H. Wen, Z. Liu, Q. Luo, C. Shi, and P. Xiao, "Designing enhanced multidimensional constellations for code-domain NOMA," *IEEE Wireless Commun. Lett.*, vol. 11, no. 10, pp. 2130–2134, 2022.
- [24] L. Yu, P. Fan, D. Cai, and Z. Ma, "Design and analysis of SCMA codebook based on Star-QAM signaling constellations," *IEEE Trans. Veh. Technol.*, vol. 67, no. 11, pp. 10 543–10 553, Aug. 2018.
- [25] Y.-M. Chen, P.-H. Wang, C.-S. Cheng, and Y.-L. Ueng, "A joint design of SCMA codebook and PTS-based PAPR reduction for downlink OFDM scheme," *IEEE Trans. Vehi. Tech.*, vol. 71, no. 11, pp. 11 936–11 948, 2022.
- [26] V. Vikas, A. Rajesh, K. Deka, and S. Sharma, "A comprehensive technique to design SCMA codebooks," *IEEE Commun. Lett.*, vol. 26, no. 8, pp. 1735–1739, 2022.
- [27] U. Erez, S. Litsyn, and R. Zamir, "Lattices which are good for (almost) everything," *IEEE Trans. Inf. Theory*, vol. 51, no. 10, pp. 3401–3416, 2005.
- [28] Q. Luo, Z. Liu, G. Chen, Y. Ma, and P. Xiao, "A novel multitask learning empowered codebook design for downlink SCMA networks," *IEEE Wireless Commun. Lett.*, vol. 11, no. 6, pp. 1268–1272, 2022.
- [29] W. Yuan, N. Wu, A. Zhang, X. Huang, Y. Li, and L. Hanzo, "Iterative receiver design for FTN signaling aided sparse code multiple access," *IEEE Trans. Wireless Commun.*, vol. 19, no. 2, pp. 915–928, 2020.
- [30] Y. Liu, L. Xiang, L.-L. Yang, and L. Hanzo, "Space-time coded generalized spatial modulation for sparse code division multiple access," *IEEE Trans. Wireless Commun.*, vol. 20, no. 8, pp. 5359–5372, 2021.
- [31] V. P. Klimentyev and A. B. Sergienko, "SCMA codebooks optimization based on genetic algorithm," in *23th European Wireless Conf.*, 2017, pp. 1–6.
- [32] Altera Innovate Asia website, Presentation, "1st 5G algorithm innovation competition-env1.0-SCMA." [Online]. Available: <http://www.innovateasia.com/5G/en/gp2.html>.
- [33] G. Forney and L.-F. Wei, "Multidimensional constellations. I. introduction, figures of merit, and generalized cross constellations," *IEEE J. Sel. Areas Commun.*, vol. 7, no. 6, pp. 877–892, 1989.
- [34] Z. Liu, P. Xiao, and Z. Mheich, "Power-imbalanced low-density signatures (LDS) from eisenstein numbers," in *2019 IEEE APWCS*, 2019, pp. 1–5.
- [35] Q. Luo, Z. Liu, G. Chen, and P. Xiao, "Enhancing signal space diversity for SCMA over rayleigh fading channels," *IEEE Trans. Wireless Commun.*, pp. 1–1, 2023.